Electric Field Control of Terahertz Polarization in a Multiferroic Manganite with Electromagnons

A. Shuvaev,[1] V. Dziom,[1] Anna Pimenov,[1] M. Schiebl,[1] A. A. Mukhin,[2] A. C. Komarek,[3] T. Finger,[3] M. Braden,[3] and A. Pimenov[1]

[1]*Institute of Solid State Physics, Vienna University of Technology, A-1040 Vienna, Austria*
[2]*Prokhorov General Physics Institute, Russian Academy of Sciences, 119991 Moscow, Russia*
[3]*II. Physikalisches Institut, Universität zu Köln, 50937 Köln, Germany*

(Received 23 August 2013; published 25 November 2013)

All-electrical control of a dynamic magnetoelectric effect is demonstrated in a classical multiferroic manganite $DyMnO_3$, a material containing coupled antiferromagnetic and ferroelectric orders. Because of intrinsic magnetoelectric coupling with electromagnons a linearly polarized terahertz light rotates upon passing through the sample. The amplitude and the direction of the polarization rotation are defined by the orientation of ferroelectric domains and can be switched by static voltage. These experiments allow the terahertz polarization to be tuned using the dynamic magnetoelectric effect.

DOI: 10.1103/PhysRevLett.111.227201 PACS numbers: 75.85.+t, 75.30.Ds, 78.20.Ek, 78.20.Jq

Electric and magnetic field control of the propagation and the polarization state of terahertz radiation is one of the prerequisites for continuous progress of modern electronics. A number of recent developments in this direction have been achieved using multiferroics, i.e., materials simultaneously revealing electric and magnetic ordering [1–5]. Several multiferroics provide not only a direct coupling between static electric and magnetic properties but also give the possibility of modifying dynamic susceptibilities by external fields. Application of a static magnetic field to multiferroic materials leads to dichroism in the terahertz range [6,7] or even to more complex effects like controlled chirality [8] or directional dichroism [9–11]. Electric control of terahertz radiation is more difficult to realize, and it has been recently demonstrated in Raman scattering experiments [12].

Dynamical properties of several multiferroic materials in the terahertz range are governed by novel magnetoelectric modes called electromagnons [13–16]. Electromagnons may be defined as collective excitations of the magnetic structure which are coupled to the electric dipole moment.They may be regarded as a mixture of magnons and phonons. In orthorhombic rare earth manganites $R\mathrm{MnO}_3$ one generally observes several electromagnons in the terahertz and sub-terahertz range. A strong high-frequency mode around 2–3 THz is well understood on the basis of a symmetric Heisenberg exchange (HE) coupling [17,18] as a zone edge magnon which can be excited by an electric component of the electromagnetic radiation. A second intensive mode existing at 0.5–1 THz has been explained using the same mechanism, but including a Brillouin zone folding due to modulation of the magnetic cycloid [18,19]. In the subterahertz frequency range a series of weaker modes is observed in optical [14,20] and neutron scattering experiments [21]. These modes are explained as the magnetic eigenmodes of the spin cycloid in $R\mathrm{MnO}_3$. Some of these modes may experience an electrical dipole activity due to the relativistic Dzyaloshinskii-Moriya (DM) mechanism. Dynamic contributions due to this mechanism have been investigated both experimentally and theoretically [20,22–25]. In spite of its weakness, the DM interaction is a promising mechanism especially in application to spiral magnets as it connects static spontaneous polarization and magnetic structure [22,26]. This mechanism is responsible for the switching of ferroelectric polarization by a magnetic field and for the control of magnetic structures by electric voltage in spiral magnets [5]. It may be expected that in the frequency range where the dynamics is governed by the DM mechanism, the terahertz light will be controlled by the electric field as well. In present experiments we utilize this idea for two purposes: we obtain a direct evidence of dynamical magnetoelectric coupling within the DM electromagnon and we demonstrate a possibility to control the polarization of terahertz light by applying static electric fields.

$DyMnO_3$ is a multiferroic manganite with orthorhombic structure. The high-temperature paramagnetic state in this material transfers into an incommensurate antiferromagnetic structure below $T_N \simeq 39$ K. At lower temperatures a second phase transition into a ferroelectric phase takes place at $T_c \simeq 19$ K. By analogy to $TbMnO_3$ this phase is most probably a cycloidal antiferromagnet [27] with an incommensurate propagation vector. Below the transition to the cycloidal state $DyMnO_3$ reveals static electric polarization which is aligned along the c axis (the $Pbnm$ crystallographic setting is used throughout this Letter). This polarization is well described by the DM coupling which leads to a simple expression [26]:

$$\mathbf{P}_0 \sim \delta_{j\to j+1} \times (\mathbf{S}_j \times \mathbf{S}_{j+1}). \quad (1)$$

Here $\mathbf{S}_j$ and $\mathbf{S}_{j+1}$ are the neighbor Mn^{3+} spins within ab planes and $\delta_{j\to j+1}$ is the vector connecting them [see

Fig. 1(a)]. The spin cycloid breaks the space inversion symmetry and has two possible rotation directions of the spins (↺ and ↻). According to Eq. (1), the sign of the static polarization is opposite in these two cases. Therefore, the antiferromagnetic domains are simultaneously ferroelectric domains, and the orientation of the spin cycloid is also affected by the external electric field.

The idea of the present experiment is based on the DM coupling between static and dynamic properties in $DyMnO_3$. A schematic picture of the cycloidal magnetic structure in $DyMnO_3$ is shown in Fig. 1(a). Because of an incommensurate character of the cycloid, the solution of the dynamic equations for this structure reveals three eigenmodes (see Supplemental Material [28] for more detail). For the present experiment only one mode is the most promising. Within this mode magnetization and electric polarization oscillate along the b and a axes, respectively, [DM electromagnon in Fig. 1(a)]. Therefore, this mode can be excited either via electric channel by $e \parallel a$ or via magnetic channel by $h \parallel b$. Moreover, these two channels are not independent. The electric excitation drives also the magnetic moment and vice versa. As discussed in more detail in the Supplemental Material [28], this cross coupling is manifested in the existence of the nonzero dynamic magnetoelectric susceptibility χ^{me}_{ab}.

The main experimental difficulty in observing the dynamic magnetoelectric effect in $DyMnO_3$ is that it cannot be detected in an experiment with an ab-plane cut crystal. In such geometry the ac fields of the incident wave are either $e \parallel b$ or $h \parallel a$ and do not excite the electromagnon at

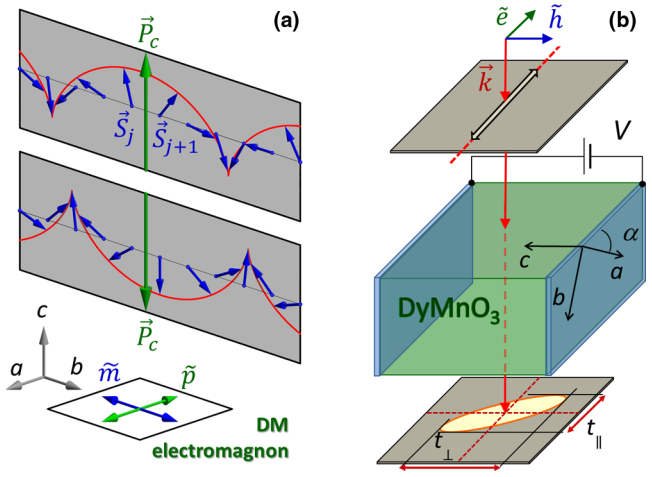

FIG. 1 (color online). Experiment to observe the electrically controlled dynamic magnetoelectric effect. (a) Schematic representation of the magnetic bc cycloid and the static electric polarization (green arrows) in $DyMnO_3$. Shown are two possible domains with opposite orientations of the cycloid and the polarization. Bottom diagram indicates oscillations of electric and magnetic moments for the magnetoelectrically active mode (DM electromagnon). (b) Geometry of the $DyMnO_3$ crystal and of the experimental apparatus to separate waves of different polarizations.

all, or they are $e \parallel a$ and $h \parallel b$ and, therefore, they both excite the electromagnon at the same time. The existence of the magnetoelectric effect in such geometry does not lead to an emergence of a wave with the perpendicular polarization but only slightly changes the absorption of light. In order to overcome this difficulty, the sample with tilted axes has to be used. The geometry of such an experiment is shown in Fig. 1(b). In the following arguments we assume an incident wave with electric field component $e \parallel ab$ plane of the crystal which excites the DM electromagnon via the electric channel. This geometry is equivalent to $e \perp c$ in Fig. 1(b) and contains both components of the electric field $e \parallel a$ and $e \parallel b$. Because the DM electromagnon has a nonzero magnetoelectric component χ^{me}_{ab}, an ac magnetic field $h \parallel b$ will be induced by this excitation. This electromagnetic field corresponds to a wave with polarization perpendicular to the incident wave with $h \parallel c$. Thus, an appearance of a signal in crossed polarizers is a characteristic of a nonzero magnetoelectric susceptibility. These qualitative arguments are supported by rigorous calculations given in the Supplemental Material [28].

We note that within the present experiment the existence of the DM electromagnon that can be excited at the center of the Brillouin zone is crucial. As shown in the rigorous solution Supplemental Eq. (5) [28], the electrically and magnetoelectrically active mode can be represented as a symmetric superposition of two magnons with wave vectors $\mathbf{q} = +\mathbf{Q}$ and $\mathbf{q} = -\mathbf{Q}$. Here, $\mathbf{Q}$ is the modulation vector of the magnetic cycloid [17]. The symmetric mode represents an electromagnon which has nonzero dynamic polarization along the x axis and, therefore, can be excited by an electromagnetic wave with $e \parallel a$.

In the case of (although much stronger) Heisenberg electromagnons [17,18], which are excited as a zone edge magnons, the present experiment would not work. For the zone edge electromagnon the neighbor spins oscillate out of phase, which cancels the resulting magnetic moment. Although this mode reveals a strong electric contribution, the magnetic and magnetoelectric susceptibilities are zero. As will be shown in more detail below (Fig. 3), the dynamic magnetoelectric effects observed in $DyMnO_3$ are indeed centered around the weak DM electromagnon at 210 GHz and they are absent around the strong Heisenberg electromagnon around 550 GHz.

The remaining point is the requirement of an electrical poling of $DyMnO_3$ crystal. Without poling, two types of domains shown in Fig. 1(a) coexist in the sample. The domains with the opposite (↺ or ↻) rotation of the spin cycloid reveal the opposite sign of the magnetoelectric susceptibility, canceling the effect. In order to avoid the signal compensation from different domains, the sample has been poled in static electric fields $E \| c$. Such poling orients the majority of the domains along one direction.

Figure 2(a) shows a typical result of the experiment in crossed polarizers geometry. We note that crossed

polarizers separate the incident polarization from the induced one. As expected, no signal could be detected in the paraelectric phase. Immediately upon the onset of the ferroelectric phase, distinct polarization rotation is observed with the sign of the signal correlating with the sign of the static field [Fig. 2(a)]. Here we plot clockwise rotation of the polarization as a positive signal and the counterclockwise rotation as a negative signal. Equivalently, the positive and negative sign of $t_\perp$ reflect the 180° phase difference between the experimental signal for different signs of static electric field. No signal is observed without poling of the sample. These results demonstrate the validity of the qualitative arguments given above.

Another important result of this work is shown in Figs. 2(b) and 2(c). Here, not far from the phase transition into the ordered state, the ferroelectric domains may be switched by moderate static field. Because of the direct coupling of static and dynamic properties, the sign of the magnetoelectric susceptibility is switched as well. Therefore, in this range we can directly influence the signal

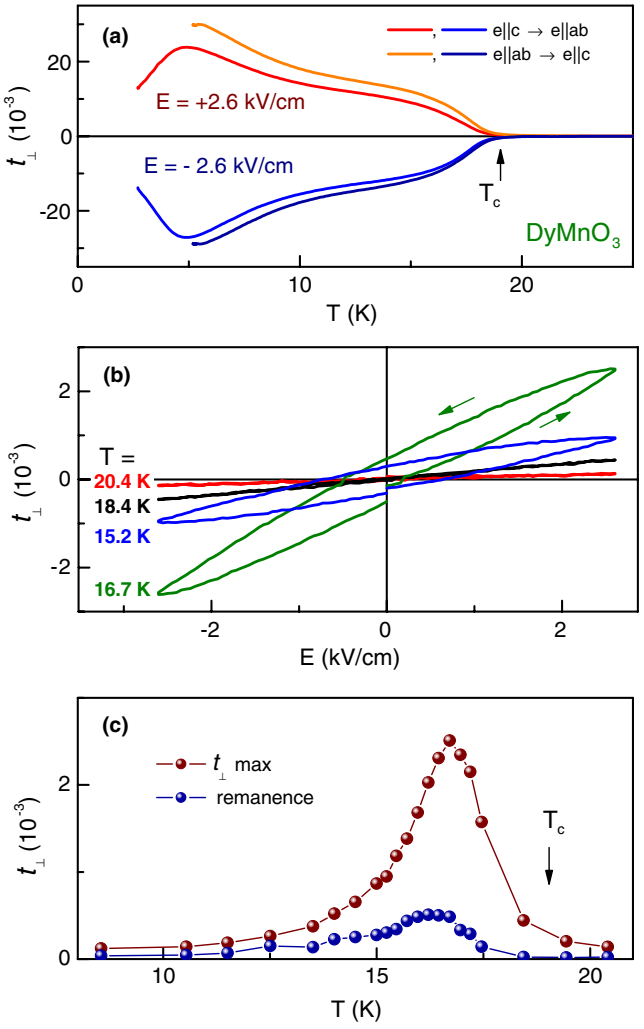

FIG. 2 (color online). Controlling of terahertz light by static electric field in $DyMnO_3$. (a) Transmitted terahertz signal in $DyMnO_3$ at $\nu = 210$ GHz in crossed polarizers for different polarizations and poling electric fields (field-cooling). The geometry of the experiment is given in Fig. 1(b). The notation $e \parallel ab$ is equivalent to $e \perp c$ in Fig. 1(b). The positive and negative signs of $t_\perp$ reflect clockwise and counterclockwise polarization rotations, respectively. Arrow indicates the phase transition to the ferroelectric phase. (b) Electric voltage dependencies of the transmission in crossed polarizers for various temperatures and for the zero-field cooled (ZFC) sample. (c) Maximum available signal in crossed polarizers and the remanence signal as a function of temperature in ZFC case. Symbols—experiment, lines are to guide the eye.

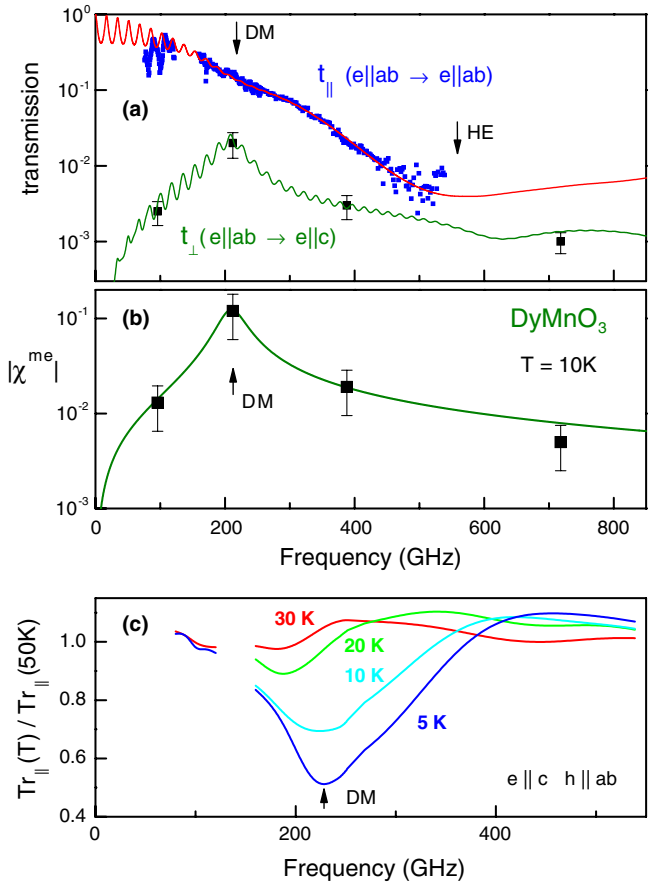

FIG. 3 (color online). Electromagnons in $DyMnO_3$. (a) Transmission spectra of $DyMnO_3$ in parallel (blue symbols) and crossed (black symbols) polarizers. The transmission is dominated by the Heisenberg electromagnon at 550 GHz (marked as HE). Much weaker Dzyaloshinskii-Moriya electromagnon (marked as DM) at 210 GHz is responsible for the observed dynamic magnetoelectric effect and for nonzero signal in crossed polarizers. Symbols—experiment, lines are fits according to the Fresnel optical equations [28]. (b) Magnetoelectric susceptibility as obtained from the spectra in (a). (c) Transmission in parallel polarizers and in the transparent geometry with $e \parallel c$ showing a magnetically excited DM electromagnon.

$t_\perp$ and the polarization rotation of the terahertz radiation by static electric field.

A significant difference between the experiments in Figs. 2(a) and 2(c) is that a field-cooling experiment is performed in the fist case and a zero-field-cooled experiment in the second case. Because in the field-cooled case the sample is cooled starting from the paraelectric state, it is much easier to align the ferroelectric domains by static field. In the zero-field-cooled sample the electric domains are not oriented. Especially at low temperatures the coercive field is strong and the static electric field cannot reorient the domains. The reorientation of the domains takes place close to the ferroelectric transition only, which explains the maxima observed in Fig. 2(c). Finally, we note that the effects in Figs. 2(a) and 2(b) are due to the same microscopic mechanism, but a direct switching of polarization in Fig. 2(b) is more relevant from the point of view of possible applications.

In order to prove the proposed mechanism of the polarization rotation, a series of spectroscopic experiments has been carried out. The terahertz dynamics in our frequency range is dominated by a strong electromagnon at about 550 GHz (18 cm^{-1}). This electromagnon is responsible for a relatively low transmission in the geometry with $e \parallel a$, seen as blue symbols in Fig. 3(a). This excitation most probably originates from a symmetric Heisenberg exchange mechanism [17,18,29] and it does not contribute to the effects described in this work.

In the transmission spectra $e \parallel a$ another weaker excitation can be seen close to 210 GHz. This mode is observed both in the geometry $e \parallel a$ [Fig. 3(a), red curve] as well as in the perpendicular geometry $e \parallel c$ [Fig. 3(c)]. In the latter geometry the sample is more transparent as the main absorption mechanism due to the Heisenberg exchange with the component $e \parallel a$ is absent. In close analogy to a similar spectral analysis [23] in $TbMnO_3$, we attribute the 210 GHz mode to the zone-center eigenmode of the cycloidal structure. This mode gets its intensity predominantly due to the Dzyaloshinskii-Moriya mechanism. Because static electric polarization is governed by the same mechanism, static and dynamic properties are strongly correlated for the 210 GHz mode. As discussed above, this connection is the basic mechanism to produce electrically controlled rotation of the terahertz polarization.

As presented in more detail in the Supplemental Material [31], the 210 GHz mode of the cycloidal spin structure reveals nonzero electric χ^e_a, magnetic χ^m_b, and magnetoelectric χ^{me}_{ab} susceptibilities. This mode can be excited by both an ac electric field $e \parallel a$ and ac magnetic field $h \parallel b$ and can be therefore called a DM electromagnon. In agreement with these arguments, a rotation of the polarization is the strongest close to 210 GHz and fades away on both sides of the resonance. This result is shown in Fig. 3(a) with black squares. The green solid line represents the result of calculations of the transmission in crossed polarizers, assuming Lorentz line shape of the DM electromagnon at 210 GHz. Tiny oscillations in this curve reflect the Fabry-Pérot resonances on the sample surfaces. In order to obtain the magnetoelectric susceptibility directly from the measured transmission, the complex transmission matrix has been inverted numerically. The frequency dependence of a resulting magnetoelectric susceptibility in $DyMnO_3$ is shown in Fig. 3(b) by black symbols. We note that in spite of the complexity of the data treatment, a nonzero signal in crossed polarizers is to a leading term directly proportional to χ^{me} [30]. This explains the qualitative similarity of the frequency dependencies of $t_\perp(\nu)$ and $\chi^{me}(\nu)$ in Figs. 3(a) and 3(b).

From the Lorentzian fits in Fig. 3 the intensities of the DM electromagnon are obtained as follows: electric contribution [Fig. 3(a)] $\Delta\varepsilon_a = 1.7 \pm 0.3$, magnetic contribution [Fig. 3(c)] $\Delta\mu_b = 0.010 \pm 0.002$, magnetoelectric contribution [Fig. 3(b)] $\Delta\chi^{me}_{ab} = 0.03 \pm 0.01$. We see that the universality condition Supplemental Material Eq. (10) [28] is not fulfilled in $DyMnO_3$: $\sqrt{\Delta\varepsilon_a \Delta\mu_b} = 0.13 > \chi^{me}_{ab}$. This disagreement most probably indicates that a large part of the DM electromagnon spectral weight is provided by the Heisenberg exchange mechanism. Indeed, a theoretical estimate of electric contribution [17] from Supplemental Eq. (8) gives the value $\Delta\varepsilon_a \sim 0.2$, substantially smaller than the experimental result.

In orthorhombic rare earth manganites ($RMnO_3$, $R =$ Dy, Tb, Eu:Y) strong zone edge electromagnons in the terahertz spectra are due to symmetric Heisenberg exchange mechanism. However, their properties do not correlate with the behavior of static electric polarization because the latter is due to antisymmetric Dzyaloshinskii-Moriya coupling. On the contrary, in present experiments static and dynamic properties are controlled by the same DM mechanism, which explains the observed voltage control of terahertz light.

Finally, the observed results differ from such well-known effect as electro-optical modulation [31] (Pockels effect). Several arguments support this statement. (i) The observed signal qualitatively follows the ferroelectric polarization [Fig. 2(a)] and disappears in the unpoled sample at low temperatures [Fig. 2(c)]. (ii) In the poling experiment the same signal is observed if only half as intensive an electric voltage is applied; i.e., the effect saturates in the field. (iii) The frequency dependence of the observed magnetoelectric signal follows the Lorentzian line shape of the DM electromagnon.

In conclusion, we investigate the dynamic magnetoelectric effect based on DM electromagnons in $DyMnO_3$. Because of the off-diagonal elements of the magnetoelectric susceptibility a polarization plane rotation of the transmitted radiation is observed. The amplitude and the direction of the polarization rotation can be controlled and switched by static electric voltage. From the spectral analysis a full set of magnetic, electric, and magnetoelectric

susceptibilities of the DM electromagnon in $DyMnO_3$ is obtained.

We thank K. Hradil for the help in sample orientation. This work was supported by the by the German Research Foundation DFG, by the Russian Foundation for Basic Researches (N 12-02-01261), and by the Austrian Science Funds (I815-N16, W1243).

[1] M. Fiebig, J. Phys. D **38**, R123 (2005).
[2] R. Ramesh and N. A. Spaldin, Nature Mater. **6**, 21 (2007).
[3] W. Eerenstein, N. D. Mathur, and J. F. Scott, Nature (London) **442**, 759 (2006).
[4] Y. Tokura, Science **312**, 1481 (2006).
[5] S.-W. Cheong and M. Mostovoy, Nature Mater. **6**, 13 (2007).
[6] A. Pimenov, A. A. Mukhin, V. Y. Ivanov, V. D. Travkin, A. M. Balbashov, and A. Loidl, Nature Phys. **2**, 97 (2006).
[7] N. Kida, S. Kumakura, S. Ishiwata, Y. Taguchi, and Y. Tokura, Phys. Rev. B **83**, 064422 (2011).
[8] S. Bordacs *et al.*, Nature Phys. **8**, 734 (2012).
[9] I. Kézsmárki, N. Kida, H. Murakawa, S. Bordács, Y. Onose, and Y. Tokura, Phys. Rev. Lett. **106**, 057403 (2011).
[10] Y. Takahashi, R. Shimano, Y. Kaneko, H. Murakawa, and Y. Tokura, Nature Phys. **8**, 121 (2012).
[11] Y. Takahashi, Y. Yamasaki, and Y. Tokura, Phys. Rev. Lett. **111**, 037204 (2013).
[12] P. Rovillain, R. de Sousa, Y. Gallais, A. Sacuto, M. A. Measson, D. Colson, A. Forget, M. Bibes, A. Barthelemy, and M. Cazayous, Nature Mater. **9**, 975 (2010).
[13] Y. Tokura and N. Kida, Phil. Trans. R. Soc. A **369**, 3679 (2011).
[14] A. M. Shuvaev, A. A. Mukhin, and A. Pimenov, J. Phys. Condens. Matter **23**, 113201 (2011).
[15] A. B. Sushkov, M. Mostovoy, R. V. Aguilar, S.-W. Cheong, and H. D. Drew, J. Phys. Condens. Matter **20**, 434210 (2008).
[16] G. A. Smolenskii and I. E. Chupis, Sov. Phys. Usp. **25**, 475 (1982).
[17] R. Valdes Aguilar, M. Mostovoy, A. B. Sushkov, C. L. Zhang, Y. J. Choi, S.-W. Cheong, and H. D. Drew, Phys. Rev. Lett. **102**, 047203 (2009).
[18] J. S. Lee, N. Kida, S. Miyahara, Y. Takahashi, Y. Yamasaki, R. Shimano, N. Furukawa, and Y. Tokura, Phys. Rev. B **79**, 180403 (2009).
[19] M. P. V. Stenberg and R. de Sousa, Phys. Rev. B **80**, 094419 (2009).
[20] A. Pimenov, A. M. Shuvaev, A. A. Mukhin, and A. Loidl, J. Phys. Condens. Matter **20**, 434209 (2008).
[21] D. Senff, N. Aliouane, D. N. Argyriou, A. Hiess, L. P. Regnault, P. Link, K. Hradil, Y. Sidis, and M. Braden, J. Phys. Condens. Matter **20**, 434212 (2008).
[22] H. Katsura, A. V. Balatsky, and N. Nagaosa, Phys. Rev. Lett. **98**, 027203 (2007).
[23] A. Pimenov, A. Shuvaev, A. Loidl, F. Schrettle, A. A. Mukhin, V. D. Travkin, V. Y. Ivanov, and A. M. Balbashov, Phys. Rev. Lett. **102**, 107203 (2009).
[24] A. Cano, Phys. Rev. B **80**, 180416 (2009).
[25] D. Senff, P. Link, K. Hradil, A. Hiess, L. P. Regnault, Y. Sidis, N. Aliouane, D. N. Argyriou, and M. Braden, Phys. Rev. Lett. **98**, 137206 (2007).
[26] M. Mostovoy, Phys. Rev. Lett. **96**, 067601 (2006).
[27] M. Kenzelmann, A. B. Harris, S. Jonas, C. Broholm, J. Schefer, S. B. Kim, C. L. Zhang, S.-W. Cheong, O. P. Vajk, and J. W. Lynn, Phys. Rev. Lett. **95**, 087206 (2005).
[28] See Supplemental Material at http://link.aps.org/supplemental/10.1103/PhysRevLett.111.227201 for details on experiment, data processing, and theory of dynamic susceptibilities of a cycloidal magnet.
[29] N. Kida, Y. Ikebe, Y. Takahashi, J. P. He, Y. Kaneko, Y. Yamasaki, R. Shimano, T. Arima, N. Nagaosa, and Y. Tokura, Phys. Rev. B **78**, 104414 (2008).
[30] A. M. Shuvaev, S. Engelbrecht, M. Wunderlich, A. Schneider, and A. Pimenov, Eur. Phys. J. B **79**, 163 (2011).
[31] L. Landau and E. Lifshitz, *Electrodynamics of Continuous Media*, Course of Theoretical Physics (Pergamon, New York, 1975).